

A Link between ER Tethering and COP-I Vesicle Uncoating

Sabrina Zink,¹ Dirk Wenzel,² Christian A. Wurm,³ and Hans Dieter Schmitt^{1,*}

¹Department Neurobiology

²Laboratory of Electron Microscopy

³Mitochondrial Structure and Dynamics Group, Department of NanoBiophotonics
Max Planck Institute for Biophysical Chemistry, Göttingen, D37077, Germany

*Correspondence: hschmit@gwdg.de

DOI 10.1016/j.devcel.2009.07.012

SUMMARY

The yeast Dsl1p vesicle tethering complex, comprising the three subunits Dsl1p, Dsl3p, and Tip20p, is stably associated with three endoplasmic reticulum-localized Q-SNAREs and is believed to play a central role in the tethering and fusion of Golgi-derived COP-I transport vesicles. Dsl1p also interacts directly with COP-I subunits. We now show that binding of Dsl1p to COP-I subunits involves binding sites identical to those involved in interactions between COP-I subunits that stabilize the COP-I coat. Cells with defects in Dsl/SNARE complex function show massive accumulation of COP-I-coated vesicles in a cluster to which COP-II coat proteins are also recruited. Our results suggest that binding of Dsl/SNARE complex to the COP-I coat complex serves two functions: to mediate vesicle tethering and to assist the uncoating process by blocking domains in COP-I that drive repolymerization and the formation of large COP-I aggregates.

INTRODUCTION

Vesicular transport involves cycles of budding and fusion catalyzed by different sets of conserved protein complexes. The formation of vesicles depends on coat complexes for collecting cargo, for driving membrane deformation, and for pinching off the vesicle. Classical coat complexes include (i) the clathrin coat, operating both in the formation of vesicles at the plasma membrane and the Golgi complex that are ultimately destined for endosomes; (ii) the COP-I coat, which forms retrograde transport vesicles on Golgi membranes; and (iii) the COP-II coat complex, which forms anterograde transport vesicles at endoplasmic reticulum (ER) exit sites (Kirchhausen, 2000; Lee et al., 2004; McNiven and Thompson, 2006). It is generally accepted that these coats are disassembled during or soon after pinching off of the transport vesicle, i.e., well before the vesicles dock and fuse with the target membrane. Disassembly of the clathrin coat is triggered by the DnaJ-like protein auxilin that recruits the chaperone Hsp70 (Lemmon, 2001). The COP coats become unstable when the small GTPases Arf1 (COP-I) or Sar1 (COP-II) are switched into their inactive state through hydrolysis of bound

GTP. The status of Sar1 and Arf1 is controlled by GTPase-activating proteins that are components of COP-I and COP-II vesicles, respectively (Randazzo and Kahn, 1994; Yoshihisa et al., 1993). Their activity is stimulated either by the addition of the outer layer of the COP-II coat, signaling the completion of coat formation (Antonny et al., 2001), or by changes in membrane curvature (Bigay et al., 2003).

The fusion of uncoated vesicles involves auxiliary steps preceding the actual mixing of the membrane bilayers. These steps are called “tethering” and “docking,” and they ensure that only the correct membranes can fuse (Cao et al., 1998; Söllner et al., 1993). SNARE proteins are the major players during docking and the final lipid mixing of membranes (Jahn and Scheller, 2006). They represent a conserved class of membrane proteins, most of which are membrane anchored by a C-terminal transmembrane domain. During docking, SNAREs anchored in the apposed membranes form extended α helices that align in parallel (Sutton et al., 1998). The structures of the SNARE complexes elucidated so far indicate that four helices are involved in SNARE complex formation (Jahn and Scheller, 2006). The release of energy that accompanies complex formation is thought to drive membrane fusion.

Tethering factors are either long rod-like homodimers or large protein complexes of up to eight subunits (Cai et al., 2007a; Kümmel and Heinemann, 2008; Whyte and Munro, 2002). Thus, they seem to be ideally suited to form a bridge between membranes. Work in recent years has shown that tethering factors and SNAREs work together very closely, and that this interplay is orchestrated by Rab/Ypt GTPases (Markgraf et al., 2007; Seals et al., 2000). So far, eight multisubunit tethering factors have been identified in yeast, each specific for one or two particular membrane fusion steps.

Although it is generally thought that only uncoated vesicles are competent for tethering and fusion, it has recently been shown that certain tethering factors exhibit specific binding to subunits of coat complexes (Andag and Schmitt, 2003; Behnia et al., 2007; Cai et al., 2007b; Zolov and Lupashin, 2005). Cai et al. (2007b) could demonstrate that an interaction between subunits of the COP-II (Sec23p) and the TRAPPI tethering complex (Bet3p) is required for the fusion of ER-derived vesicles with the Golgi.

In this study, we have focused on the Dsl1p complex as a model to help shed more light on the functional relationship between coats, tethers, and the fusion apparatus. The yeast complex consists of three large subunits, Tip20p, Dsl1p, and

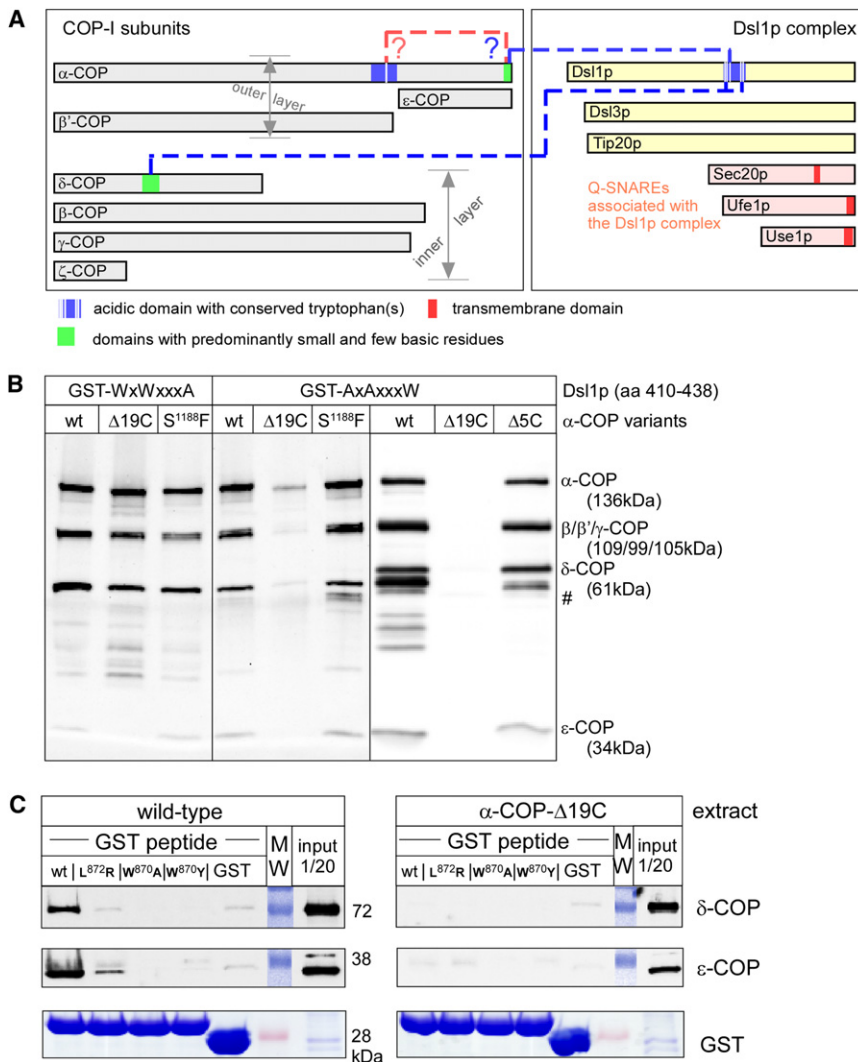


Figure 1. A Short Peptide at the C Terminus of α-COP Interacts with Dsl1p

(A) Schematic representation of the subunit composition of the COP-I complex and the Dsl1p complex. The positions of domains that are involved in interactions between the two complexes are indicated (dashed lines).

(B) GST fusions of Dsl1p-derived peptides were used in a GST pull-down assay with extracts from yeasts expressing different variants of α-COP, as indicated above each lane. The sequence of peptides fused to GST is shown in Table S1. GST-WxWxxxA was used as a control because it interacts with the δ-COP subunit of the COP-I coat, whereas GST-AxAxxxW preferentially binds to α-COP. The binding was analyzed by western blot with COP-I antibodies. The “S1188F” mutation had no effect on the interaction, because the cells had been grown at room temperature.

(C) The COP-I binding motif in Dsl1p mimics a motif in α-COP that may be used for intra-COP-I interactions. GST fusions of wild-type and mutated α-COP-derived peptides (peptides 4-7, Table S1, corresponding to sequences between residues 860 and 876) were used in a GST pull-down assay, by using extracts from wild-type cells or a *cop1*-Δ19C mutant. The binding was analyzed by western blot with COP-I antibodies. The genotypes of the yeast strains used are listed in Table S2.

Dsl3(Sec39)p, that are firmly associated with a complex of three Q-SNAREs, Ufe1p, Sec20p, and Use1p (Kraynack et al., 2005; Sweet and Pelham, 1993). In this respect, the Dsl/SNARE complex resembles very much its mammalian equivalent, the syntaxin 18 complex (Hirose et al., 2004). All six proteins are essential and play an important role in retrograde transport from the Golgi to ER, which is mediated by COP-I-coated vesicles (Andag et al., 2001; Cosson et al., 1997; Kraynack et al., 2005; Lewis and Pelham, 1996; Reilly et al., 2001; Sweet and Pelham, 1992, 1993). Previous work has shown that one of the components of the tethering complex (Dsl1p) specifically interacts with two components of the COP-I coat (Andag et al., 2001; Andag and Schmitt, 2003; Reilly et al., 2001). Although the function of these interactions is unclear, it is conceivable that Dsl1p either regulates the COP-I coat complex or that it tethers COP-I-coated vesicles directly to the target membrane.

Here, we have mapped the binding domains of Dsl1p, α-COP, and ε-COP revealing that Dsl1p binds to sites that are identical to those required for interactions between COP-I subunits

that are required for stabilization of the coat. To understand the significance of these interactions, we inactivated binding sites in Dsl1p and α-COP and analyzed “Dsl1 shut off” cells. The new *dsl1* mutants accumulate large numbers of transport vesicles. These vesicles are coated, and they form large aggregates, suggesting that uncoating and tethering/fusion are tightly linked.

RESULTS

Dsl1p and ε-COP Share the Same Binding Site in α-COP

Figure 1A shows a schematic representation of interactions between Dsl1p and COP-I proteins (dashed lines). The four binding sites highlighted in Figure 1A are two acidic tryptophan motifs, one in the center of Dsl1p and a second one around Trp870 in α-COP (blue boxes), as well as two regions located at the C terminus of α-COP and a central region within δ-COP (green boxes). The latter two regions consist mainly of small residues plus a few basic residues. The sequences are listed in Table S1 (available online). The binding sites in Dsl1p and δ-COP were described previously (Andag and Schmitt, 2003). In this work, we analyzed the binding sites in α-COP as well. Figure 1B shows GST pull-down experiments with Dsl1-derived peptides. Both peptides are variants of the wild-type sequence and either have preference to bind δ-COP (peptide WxWxxxA) or α-COP

(AxAxxxW) (Andag and Schmitt, 2003). The result of this GST pull-down experiment demonstrates that α -COP lacking the last 19 residues (Δ 1183–1291) binds less efficiently to the acidic tryptophan motif than wild-type α -COP or the *cop1*-S1188F mutant located in the same region (originally called *ret1-3*) (Duden et al., 1998). A further attempt to delineate the binding region showed that the last 5 residues of α -COP are not necessary for binding to the acidic tryptophan motif (right panel in Figure 1B). All mutants analyzed, *cop1*- Δ 19C, *cop1*-S1188F, and *cop1*- Δ 5C exhibited a growth defect at 37°C (Figure S1A). This indicates that this region has additional functions other than binding to Dsl1p.

Previous work has shown that equivalent amounts of ε -COP are required for the Dsl1p/ α -COP interaction (Andag and Schmitt, 2003), and that the last 168 residues of α -COP are required for binding ε -COP (Eugster et al., 2000). In pull-down experiments with TAP-tagged COP-I subunits presented in Figures S1B and S1C, we were able to narrow down the region required for ε -COP binding within α -COP to the 19 C-terminal residues. Thus, the same short region in α -COP is required for binding Dsl1p and ε -COP.

Dsl1p Uses a Sequence Motif for COP-I Binding that Is Present in α -COP as Well

The region around the conserved tryptophan at position 870 in α -COP resembles the α/ε -COP binding region in the center of Dsl1p (Table S1). Thus, Dsl1p may interact with the coat complex by mimicking a sequence that allows for mutual binding of α -COP subunits. To test whether the region around Trp870 in α -COP could in fact be involved in intra-COP-I interactions (red, dashed line, Figure 1A), pull-down experiments with GST-fused peptides spanning residues 860–876 of α -COP were performed (see Table S1). Three mutations were introduced into this segment to examine the specificity of binding. The cell extracts added to glutathione Sepharose loaded with these GST fusion proteins came from wild-type cells or a *cop1*- Δ 19C mutant strain. The western blot shown in Figure 1C (left panel) suggests that only the wild-type peptide is able to interact with COP-I proteins from wild-type cells. As expected, the binding efficiency was reduced when an extract from *cop1*- Δ 19C was added to the GST fusion peptides (Figure 1C, right panel).

Finally, we analyzed if the interactions observed in pull-down experiments with GST constructs expressed in *E. coli* can occur in vivo. We expressed TAP-tagged versions of Dsl1p in yeast by using the strong *GAL1* promoter and centromeric vectors. We compared wild-type *DSL1* and two mutants: (i) *ds1-1*-“W425A,” which should be unable to bind α/ε -COP, and (ii) *ds1-1*-5xWA, carrying alanine replacements of all five tryptophan residues in the COP-I binding domain (W413A, W415A, W425A, W455A, and W459A). The last mutation should affect all interactions with COP-I. Expression of the tagged proteins was induced by shifting cells to galactose medium. Proteins bound to the calmodulin Sepharose were analyzed with specific antisera directed against the smaller COP-I coat subunits δ -COP and ε -COP. Figure 2A shows that the Dsl1p/COP-I coat interactions detected by this approach are consistent with the behavior predicted from the GST pull-down experiments. Quantification of these results from three independent experiments is shown in Figure S2A. Together with our previous results, these data

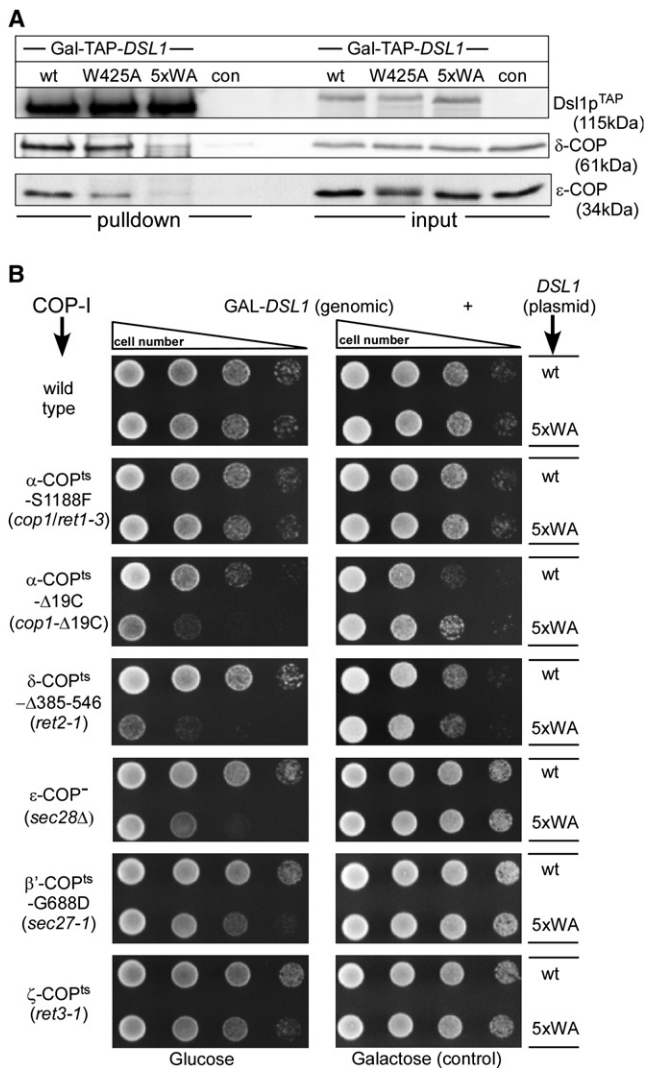
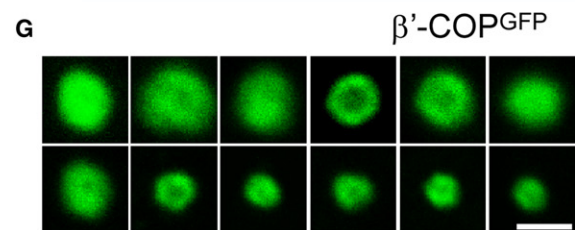
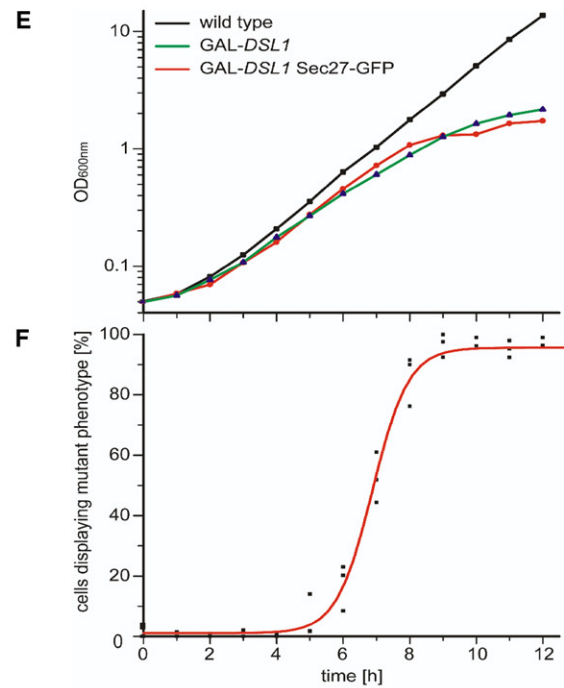
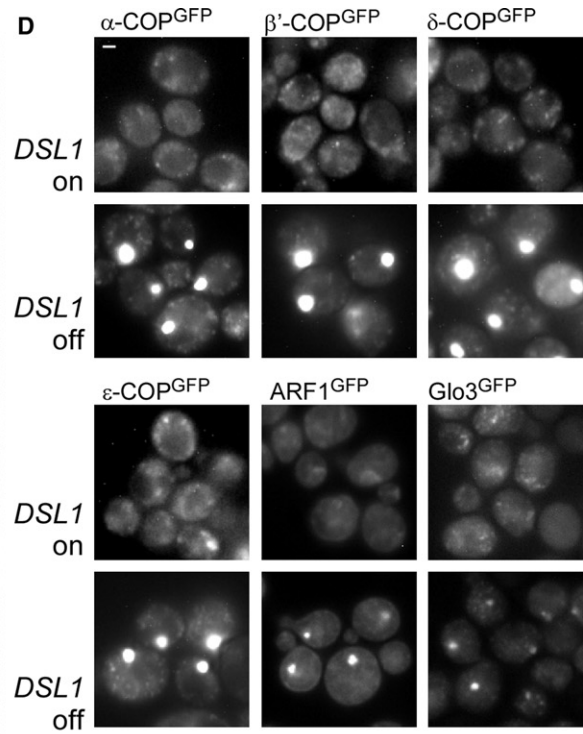
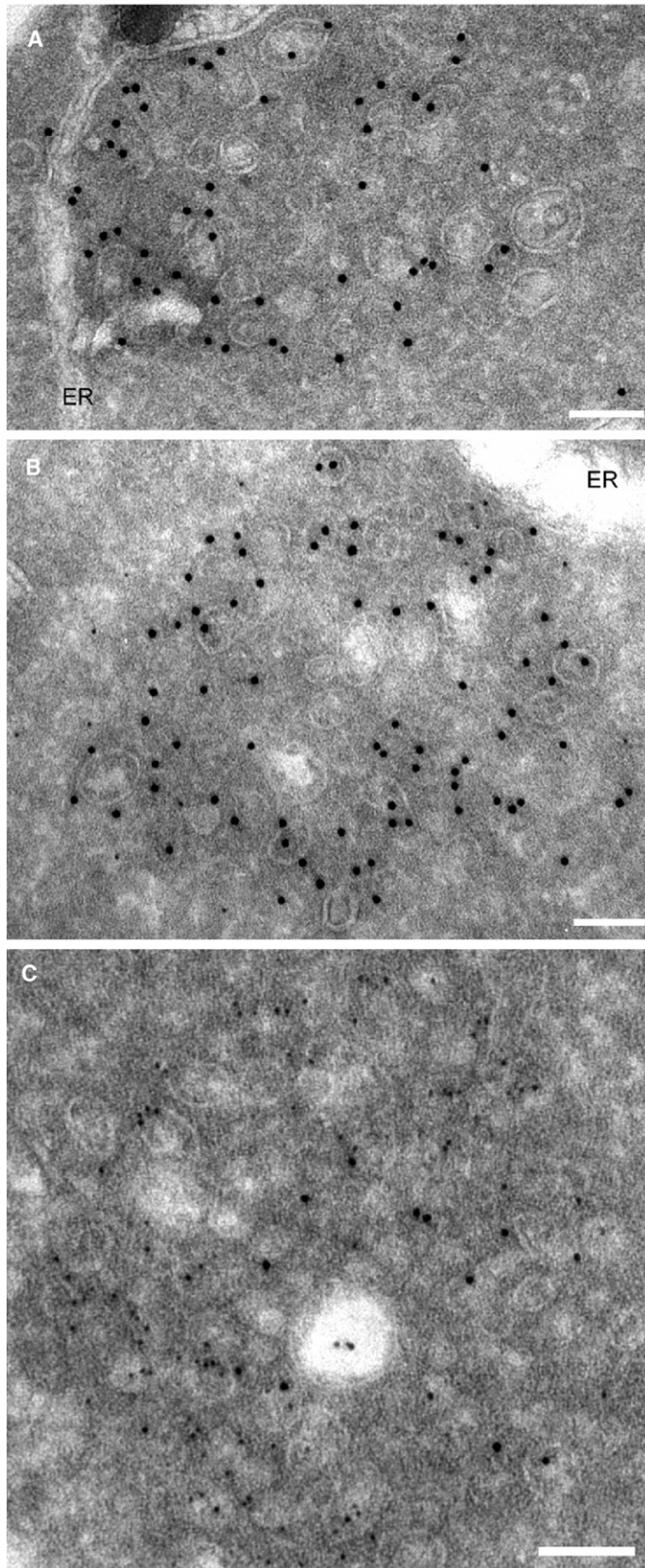


Figure 2. Mutations Affecting the Dsl1p- α -COP Interaction

(A) Affinity purification of TAP-tagged Dsl1p variants carrying mutations in the COP-I interaction domain as indicated. COP-I was partially purified from cell extracts by using calmodulin Sepharose, eluted from the resin by Laemmli buffer, and analyzed by western blot with antibodies against the COP-I complex or δ -COP and ε -COP antibodies. The strains that were used are listed in Table S2. (B) The *ds1-1*-5xWA mutation is synthetically lethal, with mutations in COP-I subunits that interact with Dsl1p. Serial dilutions of GAL-*DSL1* strains harboring mutations in different COP-I subunits as indicated at the left side of the panel. Cells were spotted on plates with selective media containing either glucose (left panels) or galactose (right panels) as the source. The galactose-containing plates (“*DSL1* on”) serve as control because they express *DSL1* from its chromosomal site, whereas, on glucose plates, cells depend on the plasmid-encoded (pRS315)-*DSL1* or *ds1-1*-5WA. The glucose plates were photographed after 2 days of incubation at 25°C, and galactose plates were photographed after 3 days at 25°C.

show that replacing all five tryptophan residues by alanine in the COP-I binding region is necessary to reduce the Dsl1p/COP-I interaction to levels below 20%.

As a second approach to investigate a possible Dsl1p/ α -COP interaction in vivo, we performed a yeast two-hybrid analysis in the presence or absence of overproduced ε -COP. The results



of this assay show that the interaction is weak but specific (Figure S2B). In summary, the data reveal an elaborate network of interactions between COP-I proteins and suggest that Dsl1p may promote or impede some of these interactions. Dsl1p uses a motif that is also present in α -COP and targets two sites in the COP-I complex involving at least three COP-I subunits.

Synthetic Effects of Mutations that Affect the Dsl1p-COP-I Interaction

Can the results of the binding studies presented above be confirmed by genetic data? To test the effect of combining *ds1* and COP-I mutations, the *ds1*-5WA mutant described above was introduced into a single-copy vector and expressed under control of its own promoter. (For information on the effects of this mutant on the growth of cells, see Figure S3 and the correction to Andag and Schmitt [2003]). Plasmids carrying wild-type and *ds1*-5xWA mutant alleles were introduced into strains with a chromosomal GAL1-*DSL1* fusion. (The effect of switching off *DSL1* on the levels of Dsl1p as well as different components of the COP-I coat and cargo molecule is illustrated in Figure S4). The strains analyzed also expressed different COP-I mutants. Thus, we were able to examine the effect of combining the *ds1*-5xWA mutation and COP-I mutants by spotting dilution cells onto glucose-containing plates. These plates were incubated at 25°C, a permissive temperature for the single mutants. In the absence of chromosomally encoded Dsl1p (Figure 2B, left panels), the combination of *ds1*-5xWA and *cop1*- Δ 19C or *ret2-1* (δ -COP) turned out to be lethal even at 25°C. Deletion of the ε -COP-encoding *SEC28* as well as point mutations in the β' -COP (*sec27-1*) and ζ -COP (*ret3-1*) genes had less dramatic effects on the growth of *ds1*-5xWA-expressing cells. The synthetic lethality observed with the *ds1*-5xWA mutation is not due to a lower stability of the 5xWA mutant protein (see legend to Figure S3B for details). In summary, *ds1*-5xWA shows strong genetic interactions with mutations in subunits of the COP-I complex that interact with Dsl1p in vitro, suggesting that the regions that were analyzed in COP-I and Dsl1p are in fact functionally related.

Clusters of Coated Vesicles Accumulate in Cells after Downregulation of the *DSL1* Gene

Next, we asked whether the coat-tether interaction examined above results in a specific phenotype when perturbed in vivo. The *ds1*-22 mutant analyzed previously lacks 30 residues in the C terminus, but leaves the COP-I binding motifs in the central region of *DSL1* intact. This mutant exhibited the typical extended

ER network like other mutants in subunits of the Dsl1p complex, but no vesicle accumulation was detected by electron microscopy (EM) (Andag et al., 2001). However, EM micrographs revealed that cells lacking the whole Dsl1 protein do accumulate vesicles (Figure 3A). Immunogold labeling with antibodies against COP-I showed that membranes at the periphery of these clusters are COP-I coated (to illustrate the specificity of the immunogold detection of COP-I subunits, an overview of a whole cell is shown in Figure S5). These vesicle clusters contain the cargo protein Emp47p (Schröder et al., 1995) (Figure 3B; Figure S10). Surprisingly, some of the membranes in these clusters could be stained with anti-Sec23p antibodies (Figure 3C). This indicated that these membrane aggregates also contain COP-II elements.

The observation that these clusters contained coated membranes was confirmed by fluorescence microscopy with “*DSL1* shut-off” cells expressing GFP-tagged coat components (Huh et al., 2003). We used C-terminally GFP-tagged versions of α -, β' -, δ -, ε -COP, Arf1p, and the retrograde Arf1-GAP Glo3p (Dogic et al., 1999; Lewis et al., 2004). In cells producing Dsl1p (either wild-type cells or GAL-*DSL1* cells grown in galactose medium), GFP-labeled COP-I gave a faint staining, with some cells showing a few weak spots. *DSL1* shut-off cells typically had one very bright spot, no matter which proteins carried the GFP tag (Figure 3D). This very intense fluorescence was not due to an increase in the amount of COP-I subunits, as shown by western blot (Figure S4A). These bright fluorescent patches are not seen in stationary cells (data not shown). In the experiments shown below, we used tagged versions of β' -COP and ε -COP, because the presence of tags had less of an effect on the growth of cells than tagged versions of α -COP and δ -COP (data not shown). Figure S5C presents evidence that Glo3p (Arf1-GAP) and COP-I proteins colocalize. Time-lapse microscopy was used to examine whether the vesicle clusters are mobile. Shortly after the *DSL1* shut-off, cells showed only weak staining with faint spots. Small bright spots appear 7 hr after switching off *DSL1*. Shortly after, this cell growth is reduced significantly (Figures 3E and 3F). These small spots moved quite rapidly within the cells. The larger vesicle clusters appearing later after the *DSL1* shut-off were less mobile or even stationary (Movies S1–S5). To evaluate the size and shape of these structures, we randomly selected a number of cells expressing β' -COP-GFP with one bright GFP spot (Figure 3G). Using confocal microscopy, their size was estimated to be below 1 μ m, which is consistent with the EM data. Most spots showed

Figure 3. Vesicles Accumulating in Dsl1p-Depleted Cells Form One Prominent Cluster

- (A) Immuno-EM of vesicles accumulating in Dsl1p-depleted cells. Strain X-64 (GAL-*DSL1*) was grown in YPD medium overnight at 30°C. Cells were fixed and prepared for analysis as described in Experimental Procedures. Slices were stained with anti-COP-I and protein A-gold (10 nm). The scale bar represents 100 nm.
- (B) Section from the same sample as in (A) labeled in addition with Emp47p antibodies and protein A-gold (5 nm).
- (C) Double immuno-EM labeling of a Dsl1p-depleted cell with Sec23p (10 nm gold) and COP-I antibodies (5 nm gold). The scale bar represents 100 nm. The scale bar represents 100 nm.
- (D) Fluorescence micrographs of GAL-*DSL1* cells expressing different GFP-tagged versions of COP-I subunits as well as Arf1p and the Arf1-GAP Glo3p. Upper panels: cells were grown overnight at 30°C in galactose-containing medium (*DSL1* on); lower panels, cells were grown overnight at 30°C in glucose-containing medium (*DSL1* off).
- (E) Growth of wild-type and GAL-*DSL1* cells (with or without GFP-tagged β' -COP) in glucose medium (YPD) at 30°C.
- (F) Time course of vesicle cluster formation after the transfer of GAL-*DSL1* cells into glucose medium (YPD). Also see the Supplemental Movies.
- (G) Vesicle clusters analyzed with a confocal microscope. Twelve random clusters in cells containing a single β' -COP positive spot were analyzed. The scale bar represents 1 μ m.

a pronounced localization of β' -GFP at their rim and a (partly) hollow interior. These spherical structures resembled the ring-like immunogold labeling of vesicle clusters often seen in the immuno-EM pictures.

In most cells, the aggregation of COP-I vesicles was reversible. Even after overnight incubation in glucose-containing medium the bright patches disappeared when cells were placed back into galactose-containing medium to switch on *DSL1* expression (Figure S4B). Within 3 hr, the number of cells containing large clusters dropped from 93% to 13%. Growth resumed after an additional 2–3 hr. At that time, 7% of the cells still exhibited the *DSL1* shut-off phenotype.

Clusters of COP-I Vesicles Accumulate in Mutants with Defects in Other Subunits of the Dsl1p Complex

We examined whether other defects in subunits of the Dsl1p complex and the associated SNAREs can also lead to the formation of vesicle clusters. For this analysis, the following mutations were combined with GFP-tagged COP-I subunits: *dsl1-22* (Andag et al., 2001), *dsl3-2* (Kraynack et al., 2005), *tip20-8* (Cosson et al., 1997), *dsl1-5xWA* (this work), *ufe1-1* (Lewis and Pelham, 1996), *sec22-3* and *sec20-1* (Novick et al., 1980), and a “SEC20 shut-off” construct (this study). As controls, we also examined four strains with defects outside the Dsl1p complex: (i) the temperature-sensitive *sec28 Δ* mutant, which lacks ϵ -COP and represents the only viable deletion of a COP-I subunit-encoding gene (Duden et al., 1998); (ii) a mutation that blocks the formation of COP-II vesicles due to a defect in the nucleotide exchange factor Sec12p for the small GTPase Sar1p (*sec12-4*) (Novick et al., 1980); and (iii) “ARF1 shut off” and “GLO3 shut off” cells (this study). The temperature-sensitive mutants were shifted from 25° to 37°C for 1.5 hr before harvesting and fixation. Cells expressing GAL-regulated genes were shifted to glucose-containing medium overnight like the GAL-*DSL1* cells. The mutants fall into three classes (Figure 4A). The first class consisted of *dsl1-22*, *sec12-4* mutants and the ϵ -COP deletion strain, which were very similar to wild-type when examined by fluorescence microscopy. The finding that *dsl1-22* showed no COP-I vesicle clustering is consistent with our previous EM studies in which we found no accumulation of vesicles (Andag et al., 2001). The *dsl3-2* and *sec22-3* mutants, members of the second class, exhibit several smaller spots containing GFP-tagged COP-I subunits. The third class, consisting of *tip20-8*, *ufe1-1*, *sec20-1* mutants and *SEC20* shut-off cells contained mostly one intense spot and very closely resembled the *DSL1*-shut off cells. Some of the mutant cells contained bright spots even when grown under permissive conditions.

A fourth group of mutants showed either very small COP-I spots, or the aggregates appeared only in a subset of cells (right-hand panel of Figure 4A). For an analysis by fluorescence microscopy, the *dsl1-5WA* mutation was integrated at the *DSL1* locus (details are presented in Figure S3A). About 10%–20% of β' -COP- or ϵ -COP-GFP-expressing *dsl1-5WA* cells exhibited large COP-I clusters. The observation that not all cells contained vesicle clusters is consistent with the notion that the mutation does not abolish the Dsl1p-COP-I interaction completely (Figure S2A). However, the result indicates that it is sufficient to disturb COP-I binding by Dsl1p to induce the accumulation of COP-I-coated vesicles in a significant number of cells.

The GAL-*ARF1* fusion was expressed from single-copy plasmids (Stearns et al., 1990) in a strain with deletions of the *ARF1* and *ARF2* genes. As shown in Figure 4A, many Arf1-depleted cells contain bright COP-I spots. However, these bright spots remained small. It has been shown that cells lacking the small GTPase Arf1p or carrying mutated Arf1 exchange factors accumulate Golgi glycosyltransferases in ring-like structures very similar to the structure shown in Figure 3G (Gaynor et al., 1998; Peyroche et al., 2001). Since these enzymes cycle through the ER, we considered that the ring structures might be to the same as the COP-I clusters observed in Dsl1p-depleted cells. However, the fact that Arf1-depleted cells contained only small COP-I spots did not confirm this possibility.

The GAL promoter was introduced at the *GLO3* site by integrating a plasmid into the genome. This also created a truncated N-terminal fragment of *GLO3* that is not functional (Schindler et al., 2009) (see Figure S3C for details). As in the case of *dsl1-5xWA* mutants, β' -COP aggregates were observed in a subset of Glo3p-depleted cells. As Glo3p is thought to be directly involved in the uncoating of COP-I vesicles, this phenotypic similarity to loss of Dsl1p complex function was striking. One should note, however, that *dsl1-5WA* mutants as well as Glo3p-depleted cells continue growing in the absence of the wild-type protein. Glo3p-depleted cells stop growing when *GCS1*, the second Arf1-GAP encoding gene, is deleted. This increased the number of Glo3p-depleted cells containing large vesicle clusters from 14% to 25% (average obtained with several different strains; SEM was 5% for both samples; see also Figure 6D). The fact that only a subset of the cells exhibit the vesicle clustering phenotype may be due to a simultaneous slow down in COP-I vesicle formation in cells lacking Glo3p (Lewis et al., 2004).

We then asked whether other mutations can prevent the accumulation of COP-I vesicles in *DSL1* shut-off cells. We combined β' -COP-GFP and GAL-*DSL1* with the *cop1- Δ 19C*, *ret2-1* (δ -COP^{ts}), and *sec28 Δ* (ϵ -COP⁻) mutations. The first two mutations prevented the formation of vesicle clusters, whereas the deletion of the *SEC28* gene had no effect (Figure 4B). Thus, ϵ -COP deletion neither causes the formation of vesicle clusters, nor interferes with cluster formation when Dsl1p is lacking. The *ret2-1* (δ -COP) allele carries a nonsense mutation that leads to a substantially truncated and unstable protein (Andag and Schmitt, 2003; Michelsen et al., 2007) and may interfere with the formation of vesicles; therefore, it may act upstream of the *DSL1* defect. In contrast, the *cop1- Δ 19C* mutation may prevent the clustering of vesicles directly.

COP-I Vesicle Clusters Contain Golgi Markers and Form Near ER Exit Sites

To identify the site at which the COP-I vesicle clusters form, we performed colocalization experiments with the Golgi markers Rer1p (early Golgi) (Boehm et al., 1994; Sato et al., 1995) and Sed7p (late Golgi) (Franzoso and Schekman, 1989). Rer1p was visualized by immunofluorescence in wild-type or *DSL1*-shut-off cells producing β' -COP-GFP. To detect Sec7p, a DsRed-tagged version of this Golgi marker (Losev et al., 2006) was introduced into a GAL-*DSL1* strain expressing GFP-tagged COP-I subunits. The colocalization of β' -COP and the transmembrane protein Rer1p was almost perfect (Figure 5A). It is likely that one fraction of the early Golgi marker became trapped in

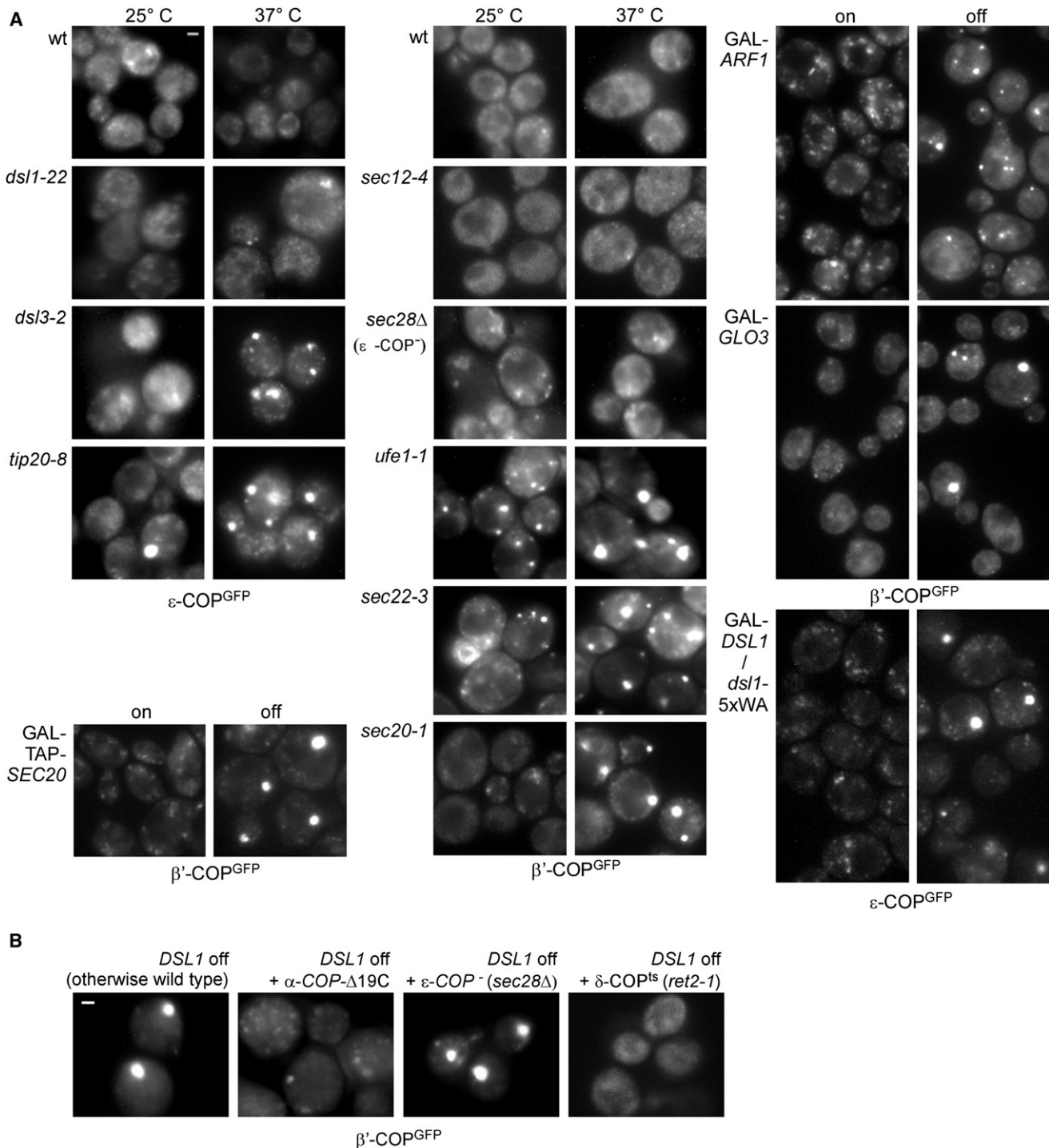


Figure 4. Defects in Different Subunits of the Dsl/SNARE Complex Can Cause Formation of Vesicle Clusters

(A) A series of wild-type cells and mutants expressing either ε-COP-GFP (*dsl1-22*, *dsl3-2*, *tip20-8*, *dsl1-5xWA*/GAL-*DSL1*) or β'-COP-GFP (*sec12-4*, *sec28Δ*, *ufe1-1*, *sec22-3*, *sec20-1*, GAL-TAP-*SEC20*, GAL-*ARF1*, GAL-*GLO3*) were analyzed by fluorescence microscopy. Cells were either grown under permissive conditions (25°C or galactose medium) or shifted to the nonpermissive temperature of 37°C for 1.5 hr. GAL-regulated expression was blocked by incubation in glucose medium overnight at 30°C.

(B) The *cop1-Δ19C* and *ret2-1* mutations prevent the formation of vesicle clusters in *DSL1* shut-off cells. The cells were grown under permissive conditions (25°C) overnight in medium containing glucose to shut-off expression of *DSL1*. The growth of the mutants we analyzed is temperature sensitive. However, we omitted the temperature shift because all mutants, including the *ret2-1* mutant, are deletion mutants (Michelsen et al., 2007).

The scale bars represent 1 μm.

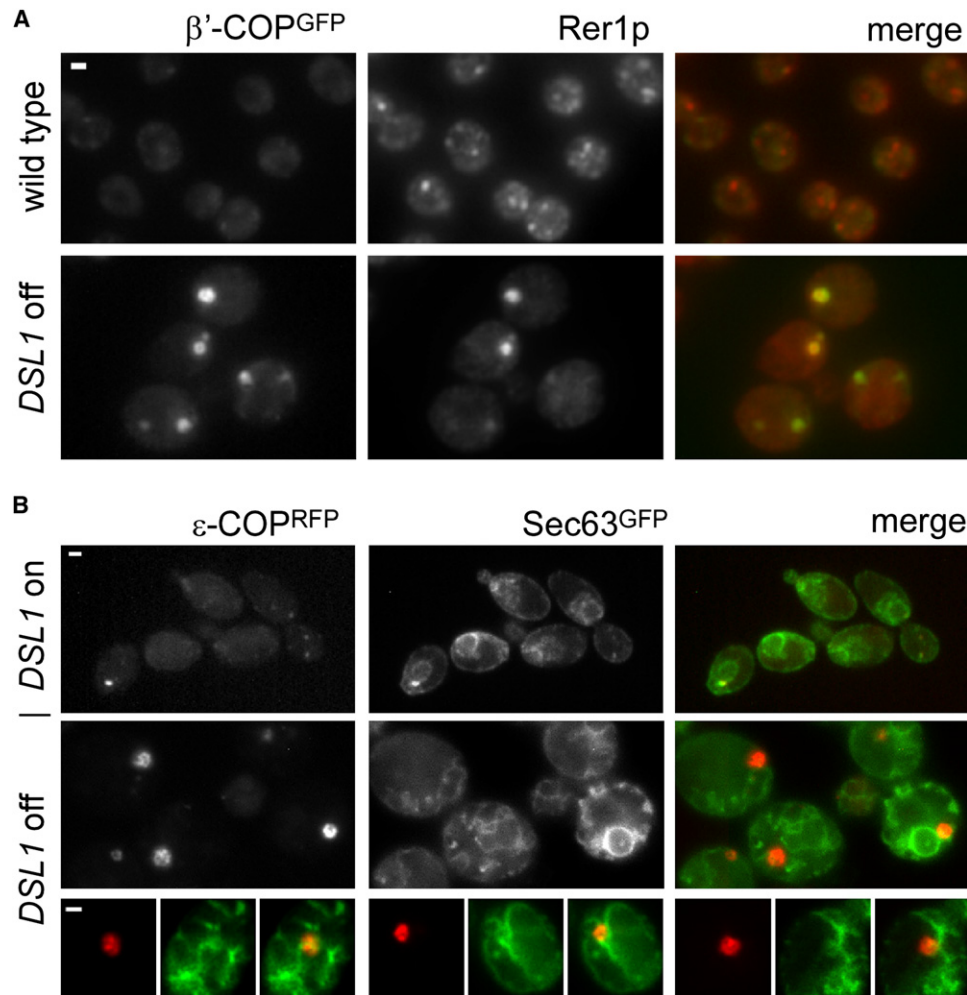


Figure 5. Vesicle Clusters in *Dsl1p*-Depleted Cells Are Close to the ER and Contain the Early-Golgi Marker Rer1p

(A and B) Fluorescence micrographs of wild-type, *DSL1* on, or *DSL1* shut-off cells. (A) Wild-type and *Dsl1p*-depleted cells were analyzed by immunofluorescence with antibodies against the early-Golgi marker Rer1p. β' -COP-GFP fluorescence was imaged as well. (B) Live images of Sec63-GFP (ER)- and ϵ -COP-RFP-expressing cells. Diploid cells (homozygous for *SEC63*-GFP and heterozygous for ϵ -COP/ ϵ -COP-RFP [RedStar]) were grown overnight at 30°C in galactose- or glucose-containing medium (*DSL1* on or *DSL1* shut-off, respectively). The scale bars represent 1 μ m.

the cluster of COP-I vesicles, whereas the rest of the molecules can be missorted to the vacuole where they are degraded. This is consistent with previous results (Boehm et al., 1994; Sato et al., 1995), and it is supported by the western blot and pull-down experiments shown in Figures S4A and S10. In contrast, Sec7p fluorescence only partially overlapped with COP-I vesicle clusters. The form of fluorescent patches and spots was very different. However, about 70% of the COP-I vesicle clusters were near Sec7p-containing structures (Figure S6).

To explore the relationship between the vesicle clusters in *DSL1* shut-off cells and the ER, we performed fluorescence microscopy with ϵ -COP-RFP and the GFP-tagged ER marker Sec63p. The most informative results were obtained with a diploid GAL-*DSL1* strain that was heterozygous for ϵ -COP/ ϵ -COP-RFP and homozygous for Sec63-GFP (Figure 5B). In “*DSL1* off” cells, COP-I aggregates were often found below the plasma membrane, very likely near the cortical ER. Figure 5B shows cells with dilated ER, which is typical for mutants with

defective *Dsl*/SNARE subunits. In these examples, most large COP-I spots are associated with the elaborate ER network. In some cells, the ER membrane seems to penetrate into holes within the vesicle clusters.

Electron microscopy had also indicated that the vesicle clusters in *DSL1* shut-off cells contain COP-II-coated membranes (Figure 3C). To test this by fluorescence microscopy, we used cells expressing combinations of m(onomeric)RFP-tagged Sec13p, a component of the COP-II outer layer and β' -COP-GFP (Figures 6A and 6B). “*DSL1* on” cells contain numerous bright COP-II-specific spots, sometimes concentrated at the nuclear envelope (Rossanese et al., 1999) (Figure 6A; Figure S7A). Nine hours after shutting off *DSL1*, larger patches of Sec13-mRFP appeared in many cells. These patches often colocalized with clusters of COP-I vesicles. There was a great variation in the composition of these mixed COP-I/II patches. With Sec13-mRFP/ β' -COP-GFP, almost perfect colocalization was observed (Figure 6A), whereas, in other combinations that were analyzed,

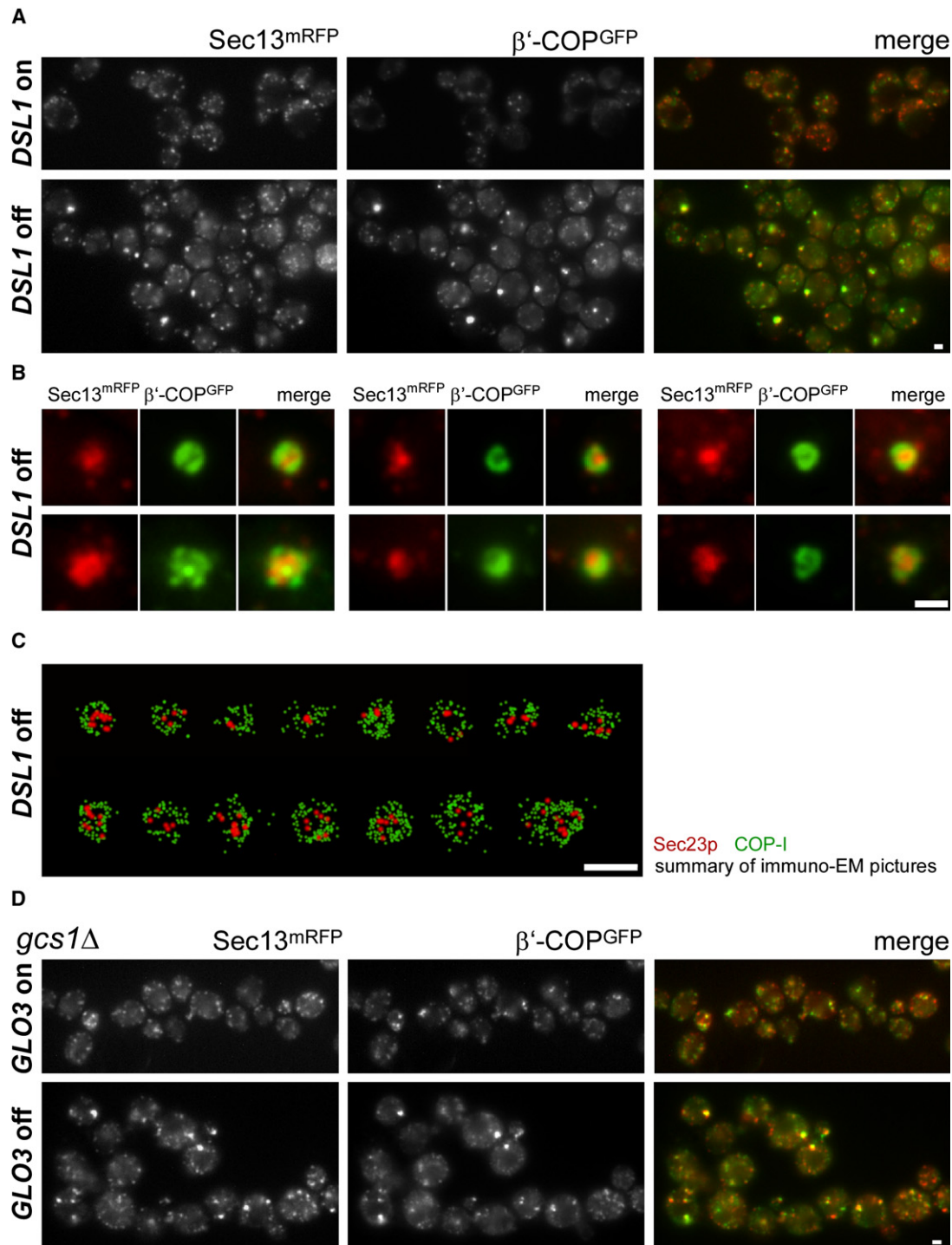


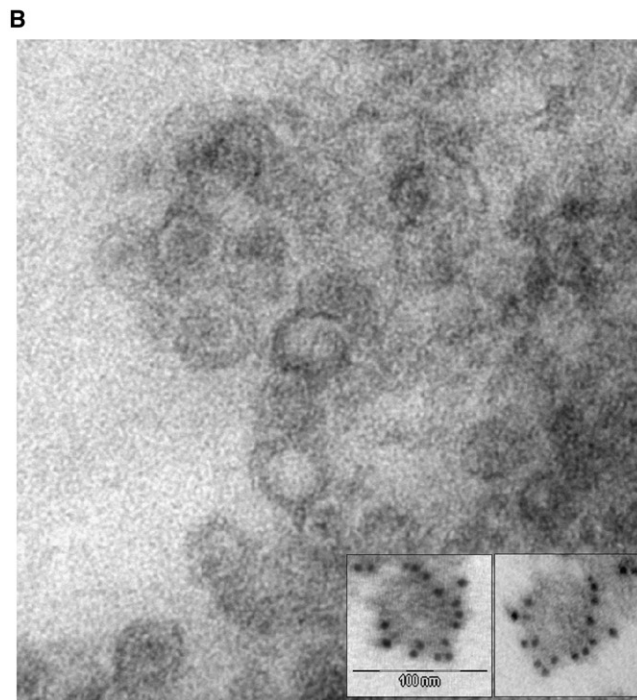
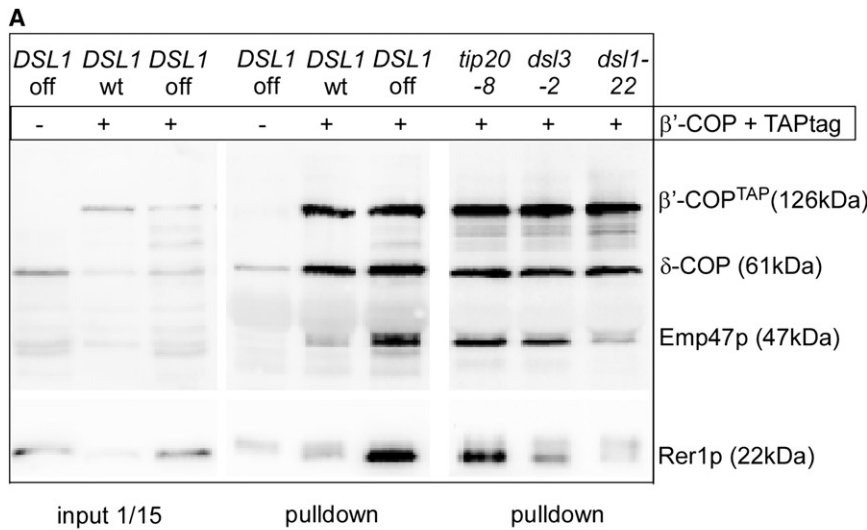
Figure 6. The COP-II Protein Sec13p Localizes to Vesicle Clusters in Dsl1p- and Glo3p-Depleted Cells

(A) Fluorescence micrographs (live images) of *DSL1* on or *DSL1* shut-off cells expressing the GFP-tagged COP-I subunit β'-COP and the COP-II subunit Sec13p carrying the monomeric RFP tag. Cells were grown overnight in galactose medium. Cultures were split, and each half was further incubated in galactose-containing medium (*DSL1* on) or glucose-containing medium (*DSL1* shut-off) for an additional 9 hr at 30°C.

(B) Details from Sec13-mRFP, β'-COP-GFP-expressing cells that were depleted of Dsl1p by overnight incubation in YPD.

(C) Summary of immuno-EM images like the one shown in Figure 3C. Fifteen images showing large clusters of COP-I vesicles were modified to make 10 nm gold (Sec23p) visible as large red spheres, whereas the 5 nm gold particles representing COP-I were replaced by green spots.

(D) β'-COP-GFP- and Sec13p-mRFP-expressing cells carrying a GAL-*GLO3* fusion and a deletion of the second Arf1-GAP encoding gene *GCS1* were transferred to glucose-containing medium and incubated overnight at 30°C (*GLO3* off). As a control, the same strain was grown in galactose-containing medium (*GLO3* on). The scale bars represent 1 μm.



~50% of the large spots contained both Sec13/31-GFP and ϵ -COP-RFP (Figures S7A and S7B). To rule out the possibility that the aggregation of COP-II-coated membranes is an artifact caused by the coexpression of two different GFP- and RFP-tagged proteins, we analyzed *Dsl1p*-depleted cells that expressed only Sec13-RFP (Figure S7C). An overlay of some vesicle clusters with a more irregular shape suggested that COP-I- and COP-II-coated membranes are close to each other but do not overlap entirely. In many instances, the darker area within the COP-I aggregates was filled with COP-II membranes. This was confirmed by an overview of immuno-EM pictures, like the one presented in Figure 3C, in which the immunogold label was replaced by colored spots (green: COP-I, red: COP-II; Figure 6C).

Figure 7. Partial Purification of Vesicles from Mutants with Defects in the *Dsl1p* Complex

(A) TAP-tagged β' -COP expressed in wild-type, *GAL-DSL1*, *tip20-8*, *dsl3-2*, or *dsl1-22* mutant cells was used to enrich COP-I and to analyze associated proteins. Temperature-sensitive mutants were shifted to 37°C for 1.5 hr before cells were harvested. Low-speed supernatants were added to IgG Sepharose beads. After incubation for 1 hr at 4°C, beads were washed and analyzed by SDS-PAGE and western blot with Emp47p, Rer1p, and δ -COP antibodies. (Note that TAP-tagged β' -COP is also recognized by the antibodies due to the protein A repeats). As a control, 1/15 of input fractions for lanes 4–6 were applied to the first three lanes.

(B) Cryosection of vesicles bound to calmodulin Sepharose from *Dsl1*-depleted cells. The inlet shows immunogold-labeled vesicles stained with COP-I antibodies. The very strong labeling is certainly due to additional binding of gold-labeled antibodies to the TAP-tagged β' -COP subunits. The scale bar represents 100 nm.

A similar dramatic aggregation of Sec13-GFP was recently observed by Castillon et al. (2009) in *sec12-4* mutant cells, mutants with a COP-II budding defect. Therefore, we examined *sec12-4/GAL-DSL1* double mutants and looked at the localization of β' -COP-GFP and Sec13-RFP that aggregate after inactivating Sec12p by a temperature shift. This shift was performed at different time points after depleting cells of *Dsl1p* by transfer to glucose-containing medium. The results shown in Figure S8 suggest that the sites of COP-I vesicle aggregation correspond to sites at which COP-II proteins accumulate in *sec12-4* mutants. Sec13-mRFP and β' -COP-GFP colocalize in Arf1-GAP-depleted cells as well (Figure 6D). Approximately 70% of the β' -COP spots show bright red fluorescence as well. Thus, defects in subunits

of the *Dsl1*/SNARE complex have similar effects on the localization of COP-I vesicles and the COP-II coat complexes as a deficiency in Arf1-GAPs, proteins thought to be directly involved in vesicle uncoating.

Analysis of Vesicles Purified from *Dsl1*-Depleted Cells

To confirm the data obtained by electron and fluorescence microscopy, and to check how tightly coat and cargo proteins are associated, we performed pull-down experiments with extracts from wild-type and mutant cells expressing tandem-affinity-tagged (TAP) β' -COP (Ghaemmaghami et al., 2003). The supernatant from low-speed centrifugations was applied to IgG Sepharose for affinity purification of coat complexes and associated structures. The middle part of Figure 7A shows that

the two Golgi-ER cargo molecules Emp47p and Rer1p (Lee et al., 2004) coprecipitate with TAP-tagged β' -COP. This observation was confirmed by sucrose gradient centrifugation with vesicle preparations from Dsl1p-depleted and wild-type cells (Figure S9A). In these gradients, a much higher portion of COP-I subunits was associated with membrane-containing fractions.

To confirm that the purified fractions indeed contained COP-I vesicles, samples from wild-type and Dsl1p-depleted cells were analyzed by electron microscopy (Figure 7B; Figure S9B). Numerous vesicles were obtained from Dsl1p-depleted cells, whereas only a few vesicles were observed when extracts from wild-type cells were applied to the affinity matrix (Figure S9B). Immunogold labeling of the beads confirmed that the surface of these beads is covered with COP-I coat proteins in both samples.

COP-I-enriched fractions from *tip20-8*, *dsl3-2*, and *dsl1-22* mutants were also analyzed by western blot with cargo-specific antibodies. In general, there is a strong correlation between the extent of vesicle clustering (Figure 4A) and the amount of cargo molecules associated with the purified COP-I subunit (Figure 7A). A comparison of partially purified COP-I and COP-II fractions from wild-type and *DSL1* shut off cells also confirmed that the COP-I- and COP-II-coated membranes do not mix and contain different cargo molecules (Figure S10). The analysis of different cargo molecules (Ste2p and Sed5p) showed that switching off *DSL1* had no effect on the association of cargo with COP-II proteins that accumulate in the clusters. Thus, it is not clear whether these sites are really ER exit sites. This is also true for the COP-II aggregates observed in *sec12-4* mutants (Castillon et al., 2009). In summary, two different approaches show that coated vesicles accumulate in mutants with malfunctioning Dsl1p subunits.

DISCUSSION

EM micrographs have shown that the most prominent phenotype of mutants with defects in subunits of the Dsl/SNARE complex is the accumulation of a dilated ER that forms an extensive network (Kaiser and Schekman, 1990; Kraynack et al., 2005; Sweet and Pelham, 1992, 1993). In addition, clusters of vesicles were observed in *SEC20* shut-off and *TIP20* shut-off cells (Sweet and Pelham, 1992, 1993). The results presented here suggest that the clusters contain coated vesicles. The fact that defects within the Dsl1p tethering complex as well as its associated SNAREs can lead to the formation of large vesicle clusters confirms that the Dsl/SNARE complex acts as a stable entity at the ER (Kraynack et al., 2005). According to a model proposed by Tripathi et al. (2009), the Dsl/SNARE complex resembles pliers whose proximal arms, Tip20p and Dsl3 (Sec39)p, are held in position by the SNAREs Sec20p and Use1p. Dsl1p constitutes the distal part of the arms and exposes in its center the unstructured domain. This domain is ideally positioned to interact with coat complexes of COP-I vesicles and constitutes the active part of this tool.

The vesicle clusters in cells with defective Dsl/SNARE complex may represent cellular structures that exist in wild-type cells either as very small or transient entities. In *DSL1* shut off cells, the formation of these clusters coincides well with the slow down of growth and is not the result of a prolonged incubation under stress conditions. Furthermore, the vesicle aggregates disperse quite rapidly after turning on the expression of *DSL1*

again. The vesicles within these clusters seem to be functional since they contain cargo molecules that are known to cycle between the Golgi and ER. Their close proximity to the ER (Figure 5B), as well as the presence of COP-II-coated membranes in their center (Figure 6), is indicative of the ER-Golgi intermediate compartment (ERGIC or VTC [vesicular tubular cluster]), as it can be found in mammalian cells (Appenzeller-Herzog and Hauri, 2006; Saraste and Svensson, 1991). Whereas the ERGIC is quite stable in mammalian cells, it seems to be very short-lived in yeast (Ben-Tekaya et al., 2005; Morin-Ganet et al., 2000).

Our results indicate that the formation of COP-I vesicle aggregates is accompanied by a recruitment of COP-II subunits to membranes in the center of the COP-I aggregates. The formation of COP-II aggregates can also be induced in *sec12-4* cells (Castillon et al. (2009). This, in turn, does not automatically lead to a comparable aggregation of COP-I vesicles (Figure 4A; Figure S8). Both types of aggregates develop at equivalent sites. They are not associated with the spindle pole body, the microtubule-organizing center in yeast (data not shown). The fact that both aggregates form at corresponding sites indicates that the COP-II spots are the result of a deficit in cargo receptors that are trapped in the COP-I vesicles. This is consistent with the observation that some *dsl1* defects can be suppressed quite efficiently by overproducing the important cargo receptor Erv14p (Powers and Barlowe, 2002; Castillon et al., 2009; VanRheenen et al., 2001).

The fact that COP-I and -II elements are very close in the mutants is also in line with observations made with *tip20-8* cells carrying a conditional lethal mutant that resembles the *DSL1* shut off cells. Kamena and Spang (2004) have shown that the *tip20-8* mutation causes a short-cut in their "round trip assay," which reconstitutes ER-Golgi anterograde and retrograde transport. Interestingly, *dsl1-22*, a mutant that does not form COP-I clusters at restrictive temperature, did not exhibit this very fast recycling. Thus, there may be a correlation between the appearance of COP-I- and COP-II-containing structures under fully restrictive conditions and the fast recycling of cargo with ER retention signals in *in vitro* experiments.

Is the Dsl1p/COP-I Coat Interaction Involved in Targeting and/or Uncoating?

The fact that coated vesicles accumulate in mutants carrying defects in the fusion machinery is in line with recent findings that suggest a role for coat complexes in vesicle targeting. This would require a longer residence time of coat complexes on newly formed vesicles than previously anticipated. A short lifetime of coats on vesicles is indicated by the finding that the Sar1/Arf1 GTPases are stimulated by factors that signal the completion of vesicle formation (Antonny et al., 2001; Bigay et al., 2003). However, it is not known how long coat complexes can persist on vesicles after GTP is hydrolyzed (Presley et al., 2002). Persistent coats may encounter tethers on the target membrane. Coat/tether interactions consistent with this scenario were found in the case of the COP-II coat and the Golgi tethers TRAPPI and Grh1p in yeast, as well as COP-I and the Golgi tethering complex COG in both yeast and mammalian cells (Behnia et al., 2007; Cai et al., 2007b; Zolov and Lupashin, 2005). The physical and genetic interactions between Dsl1p and COP-I are very complex (Figures 1 and 2; Figure S1) (Andag and Schmitt,

2003). Dsl1p binds segments within the COP-I subunits that may have a central role in the polymerization and depolymerization of the COP-I coat complex (Duden et al., 1998; Lowe and Kreis, 1996). Thus, the very complex pattern of interactions between Dsl1p and COP-I subunits may reflect the difficult task of coordinating tethering and uncoating.

Are the effects of Dsl1p depletion comparable to the results of a direct block in uncoating? Components within the COP coats that trigger their shedding are the GTPases Sar1 or Arf1 in conjunction with specific GTPase-activating proteins. Accordingly, vesicle coats can be stabilized by the addition of AIF₄ to whole cells or by the addition of nonhydrolyzable analogs of GTP as well as mutated Sar1 and Arf1 to permeabilized cells (Aridor et al., 1995; Orci et al., 1989). The result of this treatment is the accumulation of both Sec23 and β -COP at vesicular tubular clusters (Aridor et al., 1995). Similarly, we observed aggregation of COP-I and COP-II subunits in cells after shutting off the Arf1-GAPs (Figure 6D). Thus, blocking uncoating has effects on the localization of coats that are very similar to defects in the Dsl/SNARE complex in yeast (Figure 4A). However, thus far, when using vesicles purified from Dsl1p-depleted cells or *tip20-8* mutants we did not obtain evidence for an active role of the Dsl/SNARE complex in uncoating. It is likely that the Dsl/SNARE complex plays an indirect role in uncoating. COP-I vesicles may arrive at specific sites at the ER and a high concentration of COP-I complexes released at these sites may call for factors that prevent repolymerization and the aggregation of partially uncoated vesicles. In fact, partially uncoated vesicles tend to form large aggregates (Rutz et al., 2009). The role of the Dsl/SNARE may be to prevent vesicle aggregation by blocking repolymerization. Two findings support this idea. First, it is sufficient to destroy the Dsl1p/ α -COP interaction to obtain large aggregates of coated vesicles. Second, mutants lacking the putative oligomerization domain in α -COP (*cop1- Δ 19C*) do not form aggregates in Dsl1p-depleted cells. A schematic model of the Dsl1p complex operating as vesicle tether and auxiliary uncoating factor is presented in Figure S11.

The equivalent of the Dsl/SNARE complex in mammalian cells is the syntaxin 18 complex. It also functions in transport between Golgi and ER (Hirose et al., 2004; Sun et al., 2007; Aoki et al., 2009). The most obvious effect of knocking down components of the syntaxin 18 complex are dramatic changes in the morphology of Golgi (Sun et al., 2007) and ER (Nakajima et al., 2004; linuma et al., 2009). COP-I vesicles are dispersed throughout cells lacking syntaxin 18 (linuma et al., 2009). The different effects of inactivating components of the Dsl/SNARE and the syntaxin 18 complexes may be due to different modes of action of Dsl1p and its metazoan homolog ZW10. During interphase, the N terminus of ZW10 binds RINT-1 (~Tip20p), which keeps it at the ER, whereas, in mitosis, it interacts with Zwint1 and thus remains at the kinetochore to prevent premature chromosome segregation. In both phases of the cell cycle, ZW10 can switch binding partners and bind to dynamitin, a subunit of the dynein activator complex dynactin (Starr et al., 1998; Inoue et al., 2008). Thus, in interphase, ZW10 may be able to change its localization from ER to Golgi by traveling along microtubules in a dynein-dependent fashion. This implies that ZW10 can cycle between ER and Golgi, and that the ER tethering complex in higher eukaryotes is assembled from subunits present on the

vesicle and on the target membrane. In this case, the syntaxin 18 complex would resemble the exocyst tethering complex at the plasma membrane (Boyd et al., 2004). Accordingly, ZW10 lacks the COP-I binding site present in Dsl1p from yeast and in all fungi that may be required to capture vesicles. The striking accumulation of COP-I vesicles at one site within yeast mutants is certainly due to smaller distances that the vesicles must travel and the fact that the function of Dsl/SNARE complex is confined to the ER. As in other areas of cell biology, it will be interesting to compare these systems further in the future.

EXPERIMENTAL PROCEDURES

Construction of Plasmids and Strains

Strains, plasmids, and oligonucleotides are listed in Tables S2, S3, and S4, respectively. Details of plasmid and strain construction are presented in Supplemental Data. Standard procedures were used for cell growth, sporulation, and transformation. Cells expressing GAL-regulated genes were grown in rich media (YEP) or synthetic minimal (SD) media containing 2% galactose and shifted to glucose-containing media either overnight (15 hr) or for 9 hr (Figure 6) to switch off expression.

Pull-Down Experiments

GST pull-down experiments and western analysis were performed as described by Andag and Schmitt (2003). Tandem affinity purification was performed as described by Kraynack et al., (2005). No detergent was added to the buffers. Before adding the extracts to the affinity matrix, ER was removed by low-speed centrifugation (10,000 \times g). The samples used for western analysis (Figure 7A) included a single-step enrichment with IgG Sepharose (GE Healthcare). To reduce unspecific binding of COP-I proteins to IgG Sepharose, a washing step with buffer containing 300 mM instead of 150 mM NaCl was performed. To avoid unspecific COP-I binding to IgG Sepharose, calmodulin Sepharose was used in later pull-down experiments with TAP-tagged proteins. Thus, a single calmodulin Sepharose purification step was employed to enrich vesicles from 1 L cultures used for cryosections presented in Figure 7A and Figure S9B, the fractionation experiments shown in Figure S9A, as well as the experiments presented in Figure 2A and Figure S10.

Fluorescence Microscopy

Cells expressing GFP-tagged proteins alone were fixed with 4% formaldehyde for 15 min. For imaging, fixed cells were mounted in Mowiol or Dako. Since mRFP was sensitive to fixation, live cells were analyzed when colocalization of tagged proteins was determined. Cells were washed twice with water and mounted in Dako and were analyzed immediately. To avoid photoconversion of GFP to red fluorescence in living cells, red fluorescence was always recorded first (Jakobs et al., 2003). For time-lapse microscopy, living cells, grown as indicated above, were transferred to a percolation chamber that was flushed with fresh medium. To inhibit spatial movements, cells were mounted in 1% (w/v) low-melting point agarose. Imaging was performed at ambient temperature (25°C) with an epifluorescence microscope (DM6000B, Leica, Wetzlar, Germany) equipped with a Plan-Apo 100 \times 1.4 NA oil immersion objective, a GFP filter cube (excitation: 470/40 nm; emission: 525/50 nm), and a N3 filter cube (excitation: 546/12 nm; emission: 600/40 nm) (Leica). Samples presented in Figures 3D and 4–6 and Figures S5C and S6–S8 were imaged with an Axio-phot microscope equipped with the same objective using band-pass filters sets 13 and 20 (Carl Zeiss, Jena). Images were captured with a CCD camera (AxioCam MRm) by using MRGrab software (Zeiss). For confocal microscopy, we used a TCS SP5 (Leica) equipped with a Plan-Apo 63 \times 1.4 NA oil immersion objective. Excitation of GFP fusion proteins was performed with the 488 nm line of an argon ion laser. The fluorescence was detected from 500 to 625 nm. Slices from the 3D data stacks are presented. Apart from smoothing, pseudocoloring, and contrast stretching with ImageJ (NIH) or Adobe Photoshop, no further image processing was applied. For immunofluorescence, cells (3–4 OD₆₀₀ units) were fixed for 2 hr at room temperature with 3.5% formaldehyde in PBS/10% sorbitol (pH 7.0). After 2 hr of fixation at room temperature and removing the fixative by washing, cells were suspended in 100 μ l PBS/sorbitol.

To remove cell walls, samples were treated with lyticase (30 μ l of 10 μ g/ml solution) for 1 hr. Sphaeroplasts were then collected, washed four times, and resuspended in 50 μ l PBS/10% sorbitol. For details of the staining procedure with Rer1p serum and Cy3-conjugated anti-rabbit IgG (Jackson, ImmunoResearch), see work by Boehm et al. (1997).

Electron Microscopy

Ultrathin cryosections were prepared as described previously, with few modifications (Orth et al., 2007). Yeast cells were fixed with 2% formaldehyde (in 50% growth medium) for 30 min at room temperature. After centrifugation, cells were postfixed with 2% formaldehyde (in PBS) for 1 week on ice and for 2 hr with 4% formaldehyde and 0.1% glutaraldehyde. Both steps were performed on ice. Sepharose beads were fixed with 2% formaldehyde in PBS for 30 min at room temperature and postfixed with 4% formaldehyde and 0.2% glutaraldehyde for 2 hr on ice.

SUPPLEMENTAL DATA

Supplemental Data include Supplemental Experimental Procedures, eleven figures, four tables, and five movies and can be found with this article online at [http://www.cell.com/developmental-cell/supplemental/S1534-5807\(09\)00296-2](http://www.cell.com/developmental-cell/supplemental/S1534-5807(09)00296-2).

ACKNOWLEDGMENTS

We are grateful to Anne Spang, Stephan Schröder-Köhne, Uwe Andag, M. Gerard Waters, Benjamin Glick, Rainer Duden, Renwang Peng, and Dieter Gallwitz for their generous gift of reagents and advice. We thank Reinhard Jahn and Matthew Holt for valuable comments on the manuscript and Peter Mienkus for excellent technical assistance. This work was supported by the Deutsche Forschungsgemeinschaft (SFB 523).

Received: September 26, 2008

Revised: March 12, 2009

Accepted: July 3, 2009

Published: September 14, 2009

REFERENCES

Andag, U., and Schmitt, H.D. (2003). Dsl1p, an essential component of the Golgi-endoplasmic reticulum retrieval system in yeast, uses the same sequence motif to interact with different subunits of the COPI vesicle coat. *J. Biol. Chem.* *278*, 51722–51734.

Andag, U., Neumann, T., and Schmitt, H.D. (2001). The coatomer interacting protein Dsl1p is required for Golgi-to-ER retrieval in yeast. *J. Biol. Chem.* *276*, 39150–39160.

Antonny, B., Madden, D., Hamamoto, S., Orci, L., and Schekman, R. (2001). Dynamics of the COPII coat with GTP and stable analogues. *Nat. Cell Biol.* *3*, 531–537.

Aoki, T., Ichimura, S., Itoh, A., Kuramoto, M., Shinkawa, T., Isobe, T., and Tagaya, M. (2009). Identification of the neuroblastoma-amplified gene (NAG) product as a component of the syntaxin 18 complex implicated in golgi-to-endoplasmic reticulum retrograde transport. *Mol. Biol. Cell* *11*, 2639–2649.

Appenzeller-Herzog, C., and Hauri, H.P. (2006). The ER-Golgi intermediate compartment (ERGIC): in search of its identity and function. *J. Cell Sci.* *119*, 2173–2183.

Aridor, M., Bannykh, S.I., Rowe, T., and Balch, W.E. (1995). Sequential coupling between COPII and COPI vesicle coats in endoplasmic-reticulum to Golgi transport. *J. Cell Biol.* *131*, 875–893.

Behnia, R., Barr, F.A., Flanagan, J.J., Barlowe, C., and Munro, S. (2007). The yeast orthologue of GRASP65 forms a complex with a coiled-coil protein that contributes to ER to Golgi traffic. *J. Cell Biol.* *176*, 255–261.

Ben-Tekaya, H., Miura, K., Pepperkok, R., and Hauri, H.P. (2005). Live imaging of bidirectional traffic from the ERGIC. *J. Cell Sci.* *118*, 357–367.

Bigay, J., Gounon, P., Robineau, S., and Antonny, B. (2003). Lipid packing sensed by ArfGAP1 couples COPI coat disassembly to membrane bilayer curvature. *Nature* *426*, 563–566.

Boehm, J., Ulrich, H.D., Ossig, R., and Schmitt, H.D. (1994). Kex2-dependent invertase secretion as a tool to study the targeting of transmembrane proteins which are involved in ER-Golgi transport in yeast. *EMBO J.* *13*, 3696–3710.

Boehm, J., Letourneur, F., Ballensiefen, W., Ossipov, D., Demolliere, C., and Schmitt, H.D. (1997). Sec12p requires Rer1p for sorting to coatomer (COP)-coated vesicles and retrieval to the ER. *J. Cell Sci.* *110*, 991–1003.

Boyd, C., Hughes, T., Pypaert, M., and Novick, P. (2004). Vesicles carry most exocyst subunits to exocytic sites marked by the remaining two subunits, Sec3p and Exo70p. *J. Cell Biol.* *167*, 889–901.

Cai, H., Reinisch, K., and Ferro-Novick, S. (2007a). Coats, tethers, Rabs, and SNAREs work together to mediate the intracellular destination of a transport vesicle. *Dev. Cell* *12*, 671–682.

Cai, H., Yu, S., Menon, S., Cai, Y.Y., Lazarova, D., Fu, C.M., Reinisch, K., Hay, J.C., and Ferro-Novick, S. (2007b). TRAPPI tethers COPII vesicles by binding the coat subunit Sec23. *Nature* *445*, 941–944.

Cao, X.C., Ballew, N., and Barlowe, C. (1998). Initial docking of ER-derived vesicles requires Usa1p and Ypt1p but is independent of SNARE proteins. *EMBO J.* *17*, 2156–2165.

Castillon, G.A., Watanabe, R., Taylor, M., Schwabe, T.M., and Riezman, H. (2009). Concentration of GPI-anchored proteins upon ER exit in yeast. *Traffic* *10*, 186–200.

Cosson, P., Schröder-Köhne, S., Sweet, D.S., Demolliere, C., Hennecke, S., Frigerio, G., and Letourneur, F. (1997). The Sec20/Tip20p complex is involved in ER retrieval of dilysine-tagged proteins. *Eur. J. Cell Biol.* *73*, 93–97.

Dogic, D., de Chasse, B., Pick, E., Cassel, D., Lefkir, Y., Hennecke, S., Cosson, P., and Letourneur, F. (1999). The ADP-ribosylation factor GTPase-activating protein Glo3p is involved in ER retrieval. *Eur. J. Cell Biol.* *78*, 305–310.

Duden, R., Kajikawa, L., Wuestehube, L., and Schekman, R. (1998). ϵ -COP is a structural component of coatomer that functions to stabilize α -COP. *EMBO J.* *17*, 985–995.

Eugster, A., Frigerio, G., Dale, M., and Duden, R. (2000). COPI domains required for coatomer integrity, and novel interactions with Arf and Arf-GAP. *EMBO J.* *19*, 3905–3917.

Franzoso, A., and Schekman, R. (1989). Functional compartments of the yeast Golgi apparatus are defined by the sec7 mutation. *EMBO J.* *8*, 2695–2702.

Gaynor, E.C., Chen, C.Y., Emr, S.D., and Graham, T.R. (1998). Arf is required for maintenance of yeast Golgi and endosome structure and function. *Mol. Biol. Cell* *9*, 653–670.

Ghaemmaghani, S., Huh, W.K., Bower, K., Howson, R.W., Belle, A., Dephoure, N., O'Shea, E.K., and Weissman, J.S. (2003). Global analysis of protein expression in yeast. *Nature* *425*, 737–741.

Hirose, H., Arasaki, K., Dohmae, N., Takio, K., Hatsuzawa, K., Nagahama, M., Tani, K., Yamamoto, A., Tohyama, M., and Tagaya, M. (2004). Implication of ZW10 in membrane trafficking between the endoplasmic reticulum and Golgi. *EMBO J.* *23*, 1267–1278.

Huh, W.K., Falvo, J.V., Gerke, L.C., Carroll, A.S., Howson, R.W., Weissman, J.S., and O'Shea, E.K. (2003). Global analysis of protein localization in budding yeast. *Nature* *425*, 686–691.

Iinuma, T., Aoki, T., Arasaki, K., Hirose, H., Yamamoto, A., Samata, R., Hauri, H.P., Arimitsu, N., Tagaya, M., and Tani, K. (2009). Role of syntaxin 18 in the organization of endoplasmic reticulum subdomains. *J. Cell Sci.* *122*, 1680–1690.

Inoue, M., Arasaki, K., Ueda, A., Aoki, T., and Tagaya, M. (2008). N-terminal region of ZW10 serves not only as a determinant for localization but also as a link with dynein function. *Genes Cells* *13*, 905–914.

Jakobs, S., Schauss, A.C., and Hell, S.W. (2003). Photoconversion of matrix targeted GFP enables analysis of continuity and intermixing of the mitochondrial lumen. *FEBS Lett.* *554*, 194–200.

Jahn, R., and Scheller, R.H. (2006). SNAREs—engines for membrane fusion. *Nat. Rev. Mol. Cell Biol.* *7*, 631–643.

- Kaiser, C.A., and Schekman, R. (1990). Distinct sets of *SEC* genes govern transport vesicle formation and fusion early in the secretory pathway. *Cell* 61, 723–733.
- Kamena, F., and Spang, A. (2004). Tip20p prohibits back-fusion of COPII vesicles with the endoplasmic reticulum. *Science* 304, 286–289.
- Kirchhausen, T. (2000). Three ways to make a vesicle. *Nat. Rev. Mol. Cell Biol.* 1, 187–198.
- Kraynack, B.A., Chan, A., Rosenthal, E., Essid, M., Umansky, B., Waters, M.G., and Schmitt, H.D. (2005). Dsl1p, Tip20p, and the Novel Dsl3(Sec39) protein are required for the stability of the Q/t-SNARE complex at the endoplasmic reticulum in yeast. *Mol. Biol. Cell* 16, 3963–3977.
- Kümmel, D., and Heinemann, U. (2008). Diversity in structure and function of tethering complexes: evidence for different mechanisms in vesicular transport regulation. *Curr. Protein Pept. Sci.* 9, 197–209.
- Lee, M.C., Miller, E.A., Goldberg, J., Orci, L., and Schekman, R. (2004). Bi-directional protein transport between the ER and Golgi. *Annu. Rev. Cell Dev. Biol.* 20, 87–123.
- Lemmon, S.K. (2001). Clathrin uncoating: Auxilin comes to life. *Curr. Biol.* 11, R49–R52.
- Lewis, M.J., and Pelham, H.R.B. (1996). SNARE-mediated retrograde traffic from the Golgi-complex to the endoplasmic reticulum. *Cell* 85, 205–215.
- Lewis, S.M., Poon, P.P., Singer, R.A., Johnston, G.C., and Spang, A. (2004). The ArfGAP Glo3 is required for the generation of COPI vesicles. *Mol. Biol. Cell* 15, 4064–4072.
- Losev, E., Reinke, C.A., Jellen, J., Strongin, D.E., Bevis, B.J., and Glick, B.S. (2006). Golgi maturation visualized in living yeast. *Nature* 441, 1002–1006.
- Lowe, M., and Kreis, T.E. (1996). *In-vivo* assembly of coatomer, the COP-I coat precursor. *J. Biol. Chem.* 271, 30725–30730.
- Markgraf, D.F., Peplowska, K., and Ungermann, C. (2007). Rab cascades and tethering factors in the endomembrane system. *FEBS Lett.* 581, 2125–2130.
- McNiven, M.A., and Thompson, H.M. (2006). Vesicle formation at the plasma membrane and trans-Golgi network: the same but different. *Science* 313, 1591–1594.
- Michelsen, K., Schmid, V., Metz, J., Heusser, K., Liebel, U., Schwede, T., Spang, A., and Schwappach, B. (2007). Novel cargo-binding site in the β and δ subunits of coatomer. *J. Cell Biol.* 179, 209–217.
- Morin-Ganet, M.N., Rambourg, A., Deitz, S.B., Franzusoff, A., and Kepes, F. (2000). Morphogenesis and dynamics of the yeast Golgi apparatus. *Traffic* 1, 56–68.
- Nakajima, K., Hirose, H., Taniguchi, M., Kurashina, H., Arasaki, K., Nagahama, M., Tani, K., Yamamoto, A., and Tagaya, M. (2004). Involvement of BNIP1 in apoptosis and endoplasmic reticulum membrane fusion. *EMBO J.* 23, 3216–3226.
- Novick, P., Field, C., and Schekman, R. (1980). Identification of 23 complementation groups required for post-translational events in the yeast secretory pathway. *Cell* 21, 205–215.
- Orci, L., Malhotra, V., Amherdt, M., Serafini, T., and Rothman, J.E. (1989). Dissection of a single round of vesicular transport: sequential intermediates for intercisternal movement in the Golgi stack. *Cell* 56, 357–368.
- Orth, T., Reumann, S., Zhang, X., Fan, J., Wenzel, D., Quan, S., and Hu, J. (2007). The PEROXIN11 protein family controls peroxisome proliferation in *Arabidopsis*. *Plant Cell* 19, 333–350.
- Peyroche, A., Courbeyrette, R., Rambourg, A., and Jackson, C.L. (2001). The ARF exchange factors Gea1p and Gea2p regulate Golgi structure and function in yeast. *J. Cell Sci.* 114, 2241–2253.
- Powers, J., and Barlowe, C. (2002). Erv14p directs a transmembrane secretory protein into COPII-coated transport vesicles. *Mol. Biol. Cell* 13, 880–891.
- Presley, J.F., Ward, T.H., Pfeifer, A.C., Siggia, E.D., Phair, R.D., and Lippincott-Schwartz, J. (2002). Dissection of COPI and Arf1 dynamics in vivo and role in Golgi membrane transport. *Nature* 417, 187–193.
- Randazzo, P.A., and Kahn, R.A. (1994). GTP hydrolysis by ADP-ribosylation factor is dependent on both an ADP-ribosylation factor GTPase-activating protein and acid phospholipids. *J. Biol. Chem.* 269, 10758–10763.
- Reilly, B.A., Kraynack, B.A., VanRheenen, S.M., and Waters, M.G. (2001). Golgi-to-endoplasmic reticulum (ER) retrograde traffic in yeast requires Dsl1p, a component of the ER target site that interacts with a COPI coat subunit. *Mol. Biol. Cell* 12, 3783–3796.
- Rossanese, O.W., Soderholm, J., Bevis, B.J., Sears, I.B., O'Connor, J., Williamson, E.K., and Glick, B.S. (1999). Golgi structure correlates with transitional endoplasmic reticulum organization in *Pichia pastoris* and *Saccharomyces cerevisiae*. *J. Cell Biol.* 145, 69–81.
- Rutz, C., Satoh, A., Ronchi, P., Brügger, B., Warren, G., and Wieland, F.T. (2009). Following the fate in vivo of COPI vesicles generated in vitro. *Traffic* 10, 994–1005. Published online April 25, 2009. 10.1111/j.1600-0854.2009.00934.x.
- Sato, K., Nishikawa, S., and Nakano, A. (1995). Membrane-protein retrieval from the Golgi-apparatus to the endoplasmic reticulum (ER): characterization of the *RER1* gene-product as a component involved in ER localization of Sec12p. *Mol. Biol. Cell* 6, 1459–1477.
- Saraste, J., and Svensson, K. (1991). Distribution of the intermediate elements operating in ER to Golgi transport. *J. Cell Sci.* 100, 415–430.
- Schindler, C., Rodriguez, F., Poon, P.P., Singer, R.A., Johnston, G.C., and Spang, A. (2009). The GAP domain and the SNARE, coatomer and cargo interaction region of the ArfGAP2/3 Glo3 are sufficient for Glo3 function. *Traffic*, 10, 1362–1375. Published online June 9, 2009. 10.1111/j.1600-0854.2009.00952.x.
- Schröder, S., Schimmöller, F., Singer-Krüger, B., and Riezman, H. (1995). The Golgi-localization of yeast Emp47p depends on its di-lysine motif but is not affected by the *ret1-1* mutation in α -COP. *J. Cell Biol.* 131, 895–912.
- Seals, D.F., Eitzen, G., Margolis, N., Wickner, W.T., and Price, A. (2000). A Ypt/Rab effector complex containing the sec1 homolog Vps33p is required for homotypic vacuole fusion. *Proc. Natl. Acad. Sci. USA* 97, 9402–9407.
- Söllner, T., Bennett, M.K., Whiteheart, S.W., Scheller, R.H., and Rothman, J.E. (1993). A protein assembly-disassembly pathway in-vitro that may correspond to sequential steps of synaptic vesicle docking, activation, and fusion. *Cell* 75, 409–418.
- Starr, D.A., Williams, B.C., Hays, T.S., and Goldberg, M.L. (1998). ZW10 helps recruit dynactin and dynein to the kinetochore. *J. Cell Biol.* 142, 763–774.
- Stearns, T., Kahn, R.A., Botstein, D., and Hoyt, M.A. (1990). ADP ribosylation factor is an essential protein in *Saccharomyces cerevisiae* and is encoded by 2 genes. *Mol. Cell. Biol.* 10, 6690–6699.
- Sun, Y., Shestakova, A., Hunt, L., Sehgal, S., Lupashin, V., and Storrie, B. (2007). Rab6 regulates both ZW10/RINT-1- and conserved oligomeric Golgi complex-dependent Golgi trafficking and homeostasis. *Mol. Biol. Cell* 18, 4129–4142.
- Sutton, R.B., Fasshauer, D., Jahn, R., and Brunger, A.T. (1998). Crystal structure of a SNARE complex involved in synaptic exocytosis at 2.4 Å resolution. *Nature* 395, 347–353.
- Sweet, D.J., and Pelham, H.R.B. (1992). The *Saccharomyces cerevisiae* SEC20 gene encodes a membrane glycoprotein which is sorted by the HDEL retrieval-system. *EMBO J.* 11, 423–432.
- Sweet, D.J., and Pelham, H.R.B. (1993). The *TIP1* gene of *Saccharomyces cerevisiae* encodes an 80 kDa cytoplasmic protein that interacts with the cytoplasmic domain of Sec20p. *EMBO J.* 12, 2831–2840.
- Tripathi, A., Ren, Y., Jeffrey, P.D., and Hughson, F.M. (2009). Structural characterization of Tip20p and Dsl1p, subunits of the Dsl1p vesicle tethering complex. *Nat. Struct. Mol. Biol.* 16, 114–123.
- VanRheenen, S.M., Reilly, B.A., Chamberlain, S.J., and Waters, M.G. (2001). Dsl1p, an essential protein required for membrane traffic at the endoplasmic reticulum/Golgi interface in yeast. *Traffic* 2, 212–231.
- Whyte, J.R., and Munro, S. (2002). Vesicle tethering complexes in membrane traffic. *J. Cell Sci.* 115, 2627–2637.
- Yoshihisa, T., Barlowe, C., and Schekman, R. (1993). Requirement for a GTPase-activating protein in vesicle budding from the endoplasmic reticulum. *Science* 259, 1466–1468.
- Zolov, S.N., and Lupashin, V.V. (2005). Cog3p depletion blocks vesicle-mediated Golgi retrograde trafficking in HeLa cells. *J. Cell Biol.* 168, 747–759.